SLAC-PUB-15952

Observation of a Remarkable Deflection of Multi-GeV Electron Beams by a Thin Crystal

U. Wienands,* T.W. Markiewicz, J. Nelson, R.J. Noble, and J.L. Turner
SLAC National Accelerator Laboratory, 2575 Sand Hill Road, Menlo Park, California 94025

U.I. Uggerhøj and T.N. Wistisen
Dept. of Physics and Astronomy, U. of Aarhus, Ny Munkegade 120, DK-8000 Aarhus

E. Bagli, L. Bandiera, G. Germogli, V. Guidi, and A. Mazzolari
Department of Physics and Earth Sciences of the University of Ferrara, and INFN Section of Ferrara, Via Saragat 1/C, I-44122, Ferrara, Italy

R. Holtzapple and M. Miller
California Polytechnic State University, San Luis Obispo, California 93407, USA
(Dated: May 6, 2014)

We report on an experiment performing channeling and volume reflection of a high-energy electron beam using a quasimosaic Si(111) crystal at the ESTB at SLAC. The experiment used beams of 3.35 GeV and 6.3 GeV. In channeling orientation, deflections of the beam of 400 μrad with about 22% efficiency were observed, while in volume-reflection orientation, deflection of the beam by 120 μrad at 3.35 GeV and by 80 μrad at 6.3 GeV was observed with $86-95\%$ efficiency. Quantitative measurements of channeling efficiency, surface transmission and dechanneling length were taken. These are the first quantitative measurements of channeling and volume reflection using a primary beam of multi-GeV electrons.

PACS numbers: 41.85.Ct, 61.85.+p

Channeling of protons in bent crystals has been investigated for many years and has led to experiments and applications in beam extraction and beam collimation[1–6]. A wealth of data exists for protons, spanning the energy range from MeV to almost a TeV. As a consequence, proton channeling and volume reflection (VR) are reasonably well understood. Comparatively few experiments studying channeling of electrons in bent crystals have been performed, mostly with beams of relatively low energy up to about 1 GeV[7, 8] or in particle-counting experiments using secondary beams above 100 GeV[9–13] (some of which used negative pions). The reasons for this are a lack of available beams above 1 GeV for such experiments, and—being attracted to rather than repelled by the nuclei in the crystal lattice—electrons in general have less (planar) channeling efficiency than protons which makes application of bent crystals for manipulation of electron beams more challenging.

However, there is interest in the possibility of applying crystals for beam collimation of high-energy electron (and positron) beams. In the ILC[14, 15], e.g., using a short Si crystal instead of a longer amorphous spoiler would diminish wakefield effects and thus emittance dilution. Since bent crystals cause deflection of the scraped-off beam rather than scattering, an increase in collimation efficiency at reduced overall length of the system can be expected. With a bunched beam with parameters comparable to those of a high-energy collider facility this experiment can be considered a milestone experiment in studying the manipulation of electron beams with bent crystals. New initiatives towards very high energy lepton colliders[16–18] would benefit from the application of this technology as well. Application of crystals in the generation of X-rays and γ rays using electrons are holding significant promise.[19, 20] There are also a number of predictions from theory and simulations of channeling efficiency, dechanneling length and surface transmission of electrons[21] that at present can only be compared to data below 1 GeV as the high-energy experiments have not published quantitative results for these parameters. The measurements described in this paper are a first step towards improving this situation.

The Si crystal used in this experiment was fabricated at the Sensors and Semiconductor Laboratory at the University of Ferrara with crystallographic orientation chosen to produce quasimosaic bending of the (111) plane[22]. Its thickness was measured with a TMAP-4 IR interferometer to be 60 ± 1 μm. The lateral size (about 22 mm wide) was optimized in order to reduce the anticlastic deformation caused by the bending. The crystal's shape was characterized with white-light interferometry using a Veeco NT1100 Optical Profiling System, and its bending angle was measured with a Panalytical XPert PRO MRD (XL) high-resolution x-ray diffractometer. The (111) plane has a bending radius of 0.15 m for a bending angle (=channeling angle) of $\theta_c = 402 \pm 9$ μrad in the horizontal direction. The critical angle, the maximum angle a particle can have against the atomic plane for channeling to still be possible, was calculated using the Doyle-Turner potential[23] to be $\theta_{crit} = 115$ μrad at 3.35 GeV and $\theta_{crit} = 80$ μrad at 6.3 GeV. The crystal was mounted in a scattering chamber in the End Station A Test Beam[24]. A Newport AG-PR100 precision rotational stage allowed rotation of the crystal with step sizes nominally down to 5 μrad. A Newport AG-M25-27 translational stage allowed moving the crystal into the beam as well as selecting the position where the beam intercepts

Work supported in part by US Department of Energy contract DE-AC02-76SF00515,
National Science Foundation (PHY-1068662), by the Danish Council for Independent Research-Natural Sciences
FNU, and the Italian Istituto Nazionale di Fisica Nucleare (INFN) through the ICE-RAD experiment.

the crystal. A flat mirror mounted on the side of the crystal holder reflecting a laser-pointer beam to a screen at about 1 m distance provided a simple yet effective readout of the crystal angle with a resolution below 10 μrad. A YAG screen with a camera 13 m downstream of the crystal provided the main diagnostics detecting the effect of the crystal on the beam. The YAG screen camera was calibrated using the known diameter of the screen resulting in a resolution of about 28 pixels/mm in the horizontal direction; 20 pixels/mm in the vertical direction.

End station A receives beam from the SLAC linac at up to 5 pulses/sec. The optics was set to zero dispersion at the YAG screen and a beta function of 20 m at the crystal, which resulted in a beam width of < 150 μm (1σ) in the vertical and horizontal plane, after collimation. The beam divergence was inferred from wire scans taken at 8.23 m and 27.18 m downstream of the experiment to be less than 10 μrad. The momentum spread of the beam was reduced by collimation to reduce the variation in beam angle due to the unavoidable energy jitter. The intensity of the collimated beam was about 10^8 e^- per pulse. An insertable screen upstream of the crystal together with the YAG screen allowed us to maintain the beam position on the crystal at all times.

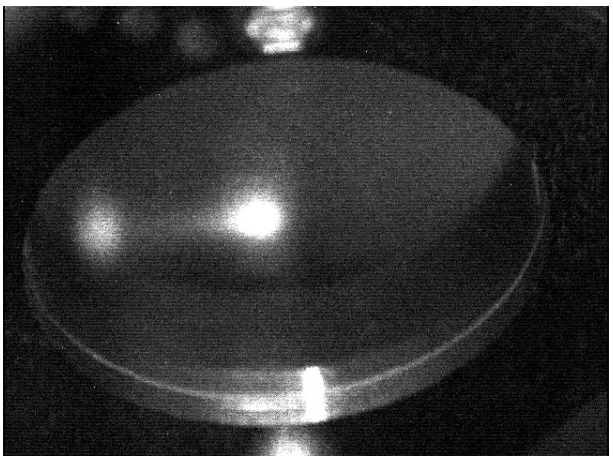

FIG. 1. YAG screen image in channeling orientation. 6.3 GeV data, contrast enhanced, not dark-frame corrected. The main peak is deliberately overexposed.

Initial setup involved rotating the crystal in the beam in larger steps until the channeling condition was satisfied, indicated by the appearance of a second beam spot on the YAG screen (Figure 1). The channeling peak is quite visible, accounting for about 20% of the intensity, as is the dechanneling tail that extends from the main peak towards the channeling peak. Volume reflection showed itself as a lateral move of essentially the whole beam to the opposite side.

The deflection plot was obtained by rotating the crystal in suitably small steps in the beam. It is shown in Fig. 2 for 6.3 GeV beam energy. From these plots, the angle for maximum channeled intensity was determined to be 400 μrad at both energies, consistent with the crystal bending angle. The volume-reflection angle is 120 μrad for 3.35 GeV and 80 μrad for 6.3 GeV beam energy.

The saved images were analyzed in ImageJ[25] and subject to a standardized data-reduction procedure. After dark-frame subtraction a 5.5° rotation was removed and the horizontal intensity profile extracted, averaging over a vertical height sufficient to cover the full extent of the beam spots. Only images with reasonable intensity were used in the analysis.

The intensity distributions obtained thus were fit with a function composed of three parts: a Gaussian each to describe the channeling peak as well as the non-deflected or volume-reflected peak, and an exponential decay describing the dechanneling tail. The dechanneling rate is taken proportional to the population of particles in the channel which leads to the exponential decay in the intensity as the beam passes through the crystal with a characteristic decay length, i.e.

$$\frac{dn(s)}{ds} = \frac{n_0}{L_d}\exp\left(-\frac{s}{L_d}\right) = \frac{n_0}{L_d}\exp\left(-\frac{\theta}{\theta_d}\right), \quad (1)$$

where n_0 is the number of particles initially in the channel, $L_d = \theta_d L_c/\theta_c$, the dechanneling length and s, the path length into the crystal; θ is the deflection angle and θ_d, the dechanneling length expressed in terms of the deflection angle. In our analysis we convolve the dechanneling tail with the multiple scattering angle. The dechanneling tail function is then

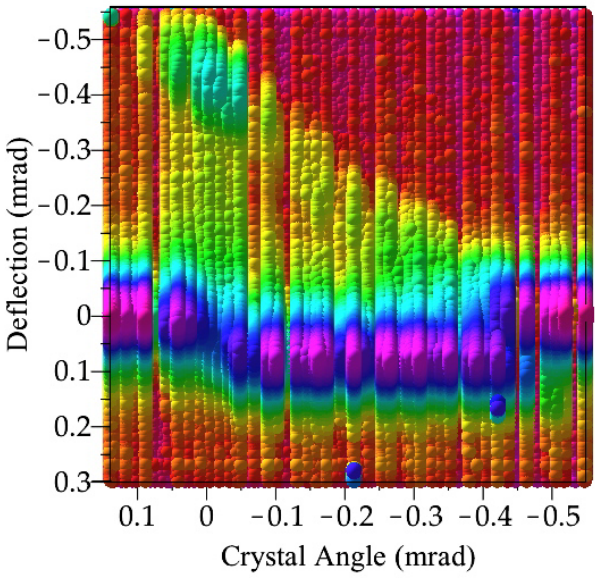

FIG. 2. (Color online) Deflection plot at 6.3 GeV beam energy. Colors correspond to log(intensity). Note that the 0 value for the crystal angle is arbitrary and does not exactly correspond to highest channeling efficiency.

$$-A_t/4\left(\mathrm{erf}\left(\frac{({\sigma_1}^2+\theta\theta_d-\theta_1\,\theta_d)}{\sqrt{2}\sigma_1\,\theta_d}\right)-1\right)\sigma_1\sqrt{\pi}\mathrm{e}^{\frac{{\sigma_1}^2+2\theta\theta_d-2\,\theta_1\,\theta_d}{2{\theta_d}^2}}\left(1+\mathrm{erf}\left(\frac{({\sigma_2}^2+\theta\theta_d-\theta_2\,\theta_d)}{\sqrt{2}\sigma_2\,\theta_d}\right)\right), \quad (2)$$

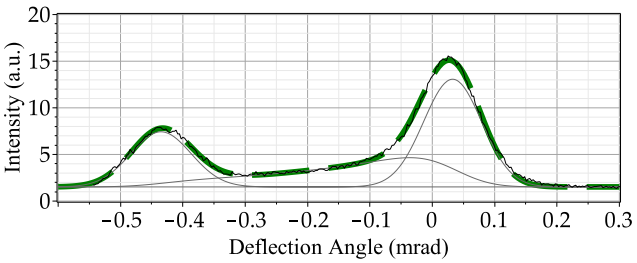

FIG. 3. (Color online) Example of the fit to 6.3 GeV channeling data. The dashed line (green) is the fitted function (green), the thin black line, the data. The solid dark-grey lines represent the individual contributions to the fit (Gaussian peaks, dechanneling tail and constant background). For this example, channeling efficiency is 23.8%, surface transmission, 55% and the dechanneling length, 33 μm.

where A_t, θ_d are the intensity and the dechanneling length of the dechanneling tail and σ_1 and σ_2, the widths of the undeflected and the channeling peak, resp. The channel is populated by the particles entering the crystal, reduced by the surface transmission (the fraction of particles initially captured in the channel). Fig. 3 shows an example of the fits obtained together with the individual contributions. Note that the fit does not constrain the area under the curves for the individual contributions with respect to each other.

From the fit parameters the following quantities are calculated:

$$\text{channeling efficiency} = \frac{\int \text{channeling peak}}{\text{total intensity}} \quad (3)$$

$$\text{surface transmission} = \frac{\int \text{channeling peak} + \text{tail}}{\text{total intensity}} \quad (4)$$

Altogether the fit involves adjusting 9 parameters: The four already mentioned, plus intensity and position for the channeling- and the undeflected or volume-reflected peak, as well as a constant background term. Correlations between the parameters can be a concern in multi-parameter fits and an effort was made to understand the correlations and their effect on the extracted numbers. The strongest correlation was identified to exist between the dechanneling length and the width of the undeflected or volume-reflected peak. There is some evidence in the data suggesting that a tail (beyond Gaussian) may exist for the undeflected or volume-reflected peak. The effect of such a tail consistent with the measured profiles was assessed to be about a 10% increase in the value of the dechanneling length extracted, which we take as an additional systematic uncertainty. The data set described here is not exhaustive enough to clearly establish presence and shape of such a tail.

The channeling efficiency is 22% at both energies with little indication of energy dependence. The VR angle, is following the expected $1/\sqrt{E}$ behavior. The experimental VR angle is essentially the same as the critical angle, somewhat in contrast to $\approx 0.8\times\theta_{crit}$ seen in other experiments with negatively charged particles[10, 27]. Surface transmission is measured to be 65% at 3.35 GeV and 57% at 6.3 GeV, in very good agreement with our analytic estimates. The dechanneling length *vs* crystal angle at 6.3 GeV is shown in Figure 4; it indicates that for the volume-captured particles (when the crystal is in VR orientation) the dechanneling length is markedly shorter, by roughly a factor of two. We suggest this may be an indication of preferential population of higher-lying energy states by the volume-captured particles, with higher probability to dechannel than the lower-lying states. Simulations in progress are consistent with this suggestion.

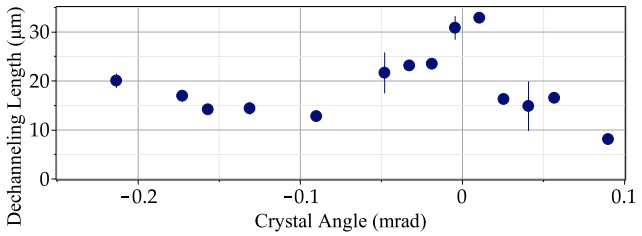

FIG. 4. (Color online) Dechanneling length *vs* crystal angle, 6.3 GeV. The horizontal scale is the same as in Fig. 2.

The VR efficiency is the content of the main (reflected) peak as a fraction of the whole intensity. This definition—using the results from our fitting procedure—gives somewhat lower numbers than one might expect, since particles identified as being in the dechanneling tail are not counted (see Fig. 3). An estimate better indicating the operationally useable VR efficiency may be a fit to the reflected peak with an asymmetric Gaussian, which includes a certain fraction of the partially reflected particles. This gives the higher numbers shown in Table I. The apparent reduction at lower energy of this number arises from the increased multiple scattering which leads to the VR peak merging with the rechanneled peak in VR orientation.

The results of the experiment are summarized in Table I.

TABLE I. Channeling parameters measured

Parameter	Unit	3.35 GeV	Simul.	6.3 GeV	Simul.
Chann. effi.	%	22 ± 1	23	22 ± 1	23
Surf. Trans.	%	64 ± 2	–	57 ± 2	–
Dech. length	μm	43 ± 6	37	$33 + 5 - 2$	42
VR deflect.	μrad	120 ± 2	100	80 ± 1	70
VR effi.	%	61 ± 2 / 86∗	77∗	63 ± 2 / 95∗	83∗

∗ Different methods of analysis, see text.

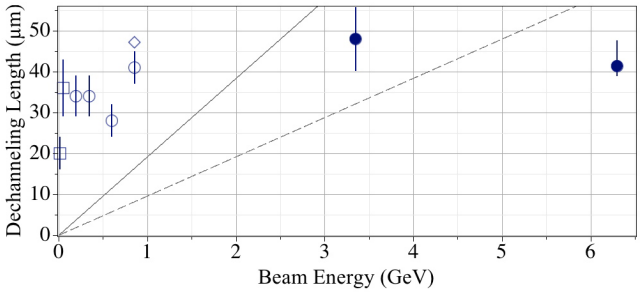

FIG. 5. (Color online) Published data for the dechanneling length of electrons in Si crystals. The two open boxes indicate data for (110) planar channeling in straight crystals[26], the open circles, (110) straight crystal[7], the open diamond, (111) straight crystal ([8], Table 1; the solid circles are this work ((111) bent crystal). Our data have been corrected for the bending angle of the crystal and the lines are using a model from[29], see text.

Figure 5 shows our results for the dechanneling length together with data from previous experiments at lower beam energies. The figure combines data from experiments with straight crystals with our data from a bent crystal. For a meaningful comparison we correct our data for this figure using the relation (see e.g. [28], eq. (7)).

$$L_{d,b} = L_{d,s}\left(1 - \frac{R_c}{R_b}\right)^2 \tag{5}$$

where $L_{d,b}$ and $L_{d,s}$ are the dechanneling length for bent and straight crystals, resp., R_b is the bending radius of 0.15 m and R_c, the Tsyganov critical radius (8 mm at 3.35 GeV and 16 mm a 6.3 GeV). This causes a 10%–20% upward scaling of our data points. This factor is not applied to the data in Table I. Also shown is a calculation using a formalism by Baier, Katkov and Strakhovenko[29] using their value of 23 eV for the potential depth U_0 which gives sensible results for proton channeling. This comparison is meaningful as the potential depth of the (110) planes and the (111) planes used here are quite comparable. In this approach, the dechanneling length scales with the inverse of the radiation length X_0. The solid, gray line indicates a calculation using the parameters for our experiment and the PDG value for X_0 in ^{28}Si, while the dashed gray line is the same calculation using half the value for X_0, as our data indicate that X_0 may be reduced for channeled electrons (see below).

There is a discrepancy between the extracted dechanneling length and surface transmission and the intensity in the channeling peak. At 6.3 GeV, for a dechanneling length of 33 μm there should be 16% particles left in the channel at the end of the crystal. Multiplied by the surface transmission of 57% it would follow that channeling efficiency would be less than 10% whereas we measure 22%. This indicates that the exponential model (eq. (1)) used to describe dechanneling may be overly simple. Calculations by the Frankfurt group for electron channeling at 855 MeV in Si-(110)[21] as well as Baryshevsky *et al.*[30] show that rechanneling is an important process and that a simple exponential decay is not a good description of the process. Recent measurements at Mainz[8] corroborate this. While these particular calculations were done for a different energy and channeling plane, a similar effect may happen for our conditions.

There is a detectable increase in width of the channeled beam in the vertical, non-channeling plane by roughly a factor 1.5 over the beam width in amorphous—or in VR— orientation of the crystal. Figure 6 shows the vertical profile of the channeling peak at 6.3 GeV together with the vertical distribution for volume-reflected particles. Expressing this increase in terms of the radiation length X_0 we get a reduction by a factor of $1/1.9$ at 3.35 GeV and $1/2.4$ at 6.3 GeV. This effect can be explained qualitatively by the increased probability of the channeled electrons to overlap with the nuclei of the crystal lattice; to our knowledge the result reported here is the first published, quantitative result of this kind. A recent measurement at 255 MeV using a straight crystal does not appear to show this effect[32]. We note however, that the DYNECHARM simulations described below do show a similar effect.

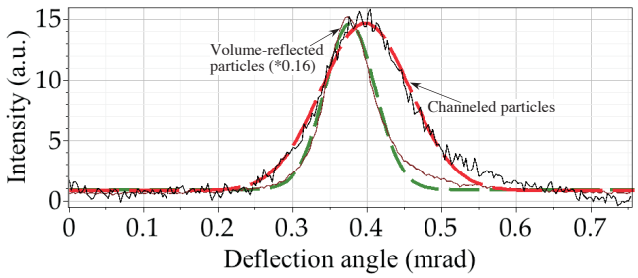

FIG. 6. (Color online) Vertical profiles of the channeled beam at 6.3 GeV. The 1-σ width of the channeled particles is 60 μrad, while the 1-σ width of the volume-reflected particles is 35 μrad, consistent with 39 μrad from the multiple-scattering formula[31]. The dashed lines are Gaussian fits

The results were compared to simulations made with the code DYNECHARM++[33], and the simulation results are included in Table I. In general, there is very good agreement between simulations and measurements. The extraction from the VR simulation data was done in a slightly different manner than for the experimental data and the differences do not point to an inconsistency. The simulation does predict somewhat lower VR angles than measured; a difference yet unexplained. A detailed comparison is beyond the scope of the present paper and planned for a later publication, but there appear to be no gross inconsistencies.

For the first time, channeling and volume reflection has been demonstrated with a full primary beam of multi-GeV electrons. The experimental data show that channeling happens with 22% efficiency and a surface transmission of $57-64\%$ for our crystal. Dechanneling length is $33-43$ μm, and up to 6.3 GeV our data indicate little or no energy dependence of the dechanneling length. There is evidence for dechanneling not being a purely exponential process and that rechanneling is an important process in determining the overall chan-

neling efficiency, as well as that the dechanneling length is shorter for rechanneled particles. Volume reflection appears to be an efficient process with effectively more than 90% of electrons found in the volume-reflected ensemble. There is evidence of increased multiple scattering when channeling, in accordance with expectation but quantitatively reported here for the first time.

The results presented here provide a first quantitative look at the processes important in channeling and VR of a high-energy electron beam and thus crucial data to further understanding and application of crystals for electron beams. The results provide important benchmark data for simulation codes; preliminary comparison to one such code indicates broad overall agreement with more detailed comparisons to follow. The results also provide data on which a first, cautious, extrapolation can be attempted to investigate the possibility of using crystal arrays in VR orientation as collimators in electron-beam machines.

ACKNOWLEDGMENTS

We would like to thank the SLAC Test Facilities Department for outstanding support in getting the experiment installed, for data acquisition support and setting up the beam line. We would like to thank G. Frequest of Fogale Nanotech (Nimes, France) for his support in measuring of crystal thickness and P. Andrea and M. Claudio of Perman (Loiano, Italy) for their support with crystal cell manufacturing. We would like to thank E.L. Bong (SLAC) for designing and building the mount for stages and crystal assembly. This work was partially supported by the US DOE under contract number DE-AC02-76SF00515, by the US National Science Foundation (PHY-1068662), by the Danish Council for Independent Research—Natural Sciences FNU, and the Italian Istituto Nazionale di Fisica Nucleare (INFN) through the ICE-RAD experiment.

* uli@slac.stanford.edu

[1] U. Uggerhøj, Rev. Mod. Phys. 77, 1131 (2005) and references therein.
[2] A.G. Afonin et al., PRST-AB 15, 081001 (2012) and references therein.
[3] W. Scandale et al., PRST-AB 11, 063501 (2008).
[4] R. Carrigan *et al.*, Phys.Rev.ST Accel.Beams 5, 043501 (2002).
[5] D. Still et al., Proc. IPAC 2012, New Orleans, Louisiana, USA, 559 (2012).
[6] R.P. Fliller III, A. Drees, D. Gassner, L. Hammons, G. McIntyre, D. Trbojevic, V. Biryukov, Y. Chesnokov, V. Terekhov, Proc. Part. Accel. Conf. Chicago, IL, (2001).
[7] W. Lauth, H. Backe, P. Kunz, A. Rueda, Int. Journal of Modern Physics A, 25, 1 136-143 (2010)
[8] A. Mazzolari *et al.*, Phys. Rev. Lett. 112, 135503 (2014).
[9] W. Scandale *et al.*, Phys. Lett. B 693 (2010) 545.
[10] W. Scandale *et al.*, Phys. Lett. B681, 233 (2009).
[11] W. Scandale *et al.*, Phys. Rev. A 79, 012903 (2009).
[12] L. Bandiera *et al.*, Nucl. Instrum. Methods B 309, 135 (2013).
[13] L. Bandiera *et al.*, Phys. Rev. Lett. 111, 255502 (2013).
[14] V.B.S. Strokov, Yu. Chesnokov, I. Endo, M. Iinuma, H. Kuroiwa, T. Ohnishi, H. Sato, S. Sawada, T. Takahashi, K. Ueda, Journal of the Physical Society of Japan 76 (2007).
[15] A. Seryi, Nucl. Instrum. Methods A 623, 23 (2010).
[16] M. Koratzinos *et al.*, Proc. Int. Part. Accel. Conf. Shanghai, CH, 1658 (2013).
[17] S. Geer, Ann. Rev. Nucl. Part. Sci. 59, 347 (2009).
[18] M.A. Palmer *et al.*, Proc. Int. Part. Accel. Conf., Shanghai, CH, 1475 (2013).
[19] B. Azadegan, W. Wagner, and J. Pawelke, Phys. Rev. B 74, 045209 (2006).
[20] W. Wagner, B. Azadegan, A. Panteleeva, J. Pawelke, and W. Enghardt, Proc. SPIE 5974, 59740B-1 (2005).
[21] G.B. Sushko, V.G. Bezchastnov, I.A. Solov'yov, A.V. Korol, W. Greiner, A.V. Solov'yov, J. Comp. Phys. 252, 404-418 (2013).
[22] V. Guidi, A. Mazzolari, D. De Salvador, and A. Carnera, Journal of Physics D-Applied Physics 42, 182005 (2009).
[23] P.A. Doyle, P.S. Turner, Acta Crystallogr. A 24, 390 (1968).
[24] `http://estb.slac.stanford.edu`
[25] W.S. Rasband, ImageJ, U. S. National Institutes of Health, Bethesda, Maryland, USA, `http://imagej.nih.gov/ij/`, 1997-2012.
[26] J.O. Kephart, R.H. Pantell, B.L. Berman, S. Datz, H. Park and R.K. Klein, Phys. Rev. B 40, 4249 (1989).
[27] A.M. Taratin, S.A. Vorobiev, Nucl. Instrum. Methods B 26, 512 (1987).
[28] A. Baurichter *et al.*, Nucl. Instrum. Meth. B164, 27 (2000).
[29] V.N. Baier, V.M. Katkov, V.M. Strakhovenko, *Electromagnetic Processes at High Energies in Oriented Single Crystals*, World Scientific, Singapore, New Jersey, London, Hong Kong (1998).
[30] V.G. Baryshevsky and V.V. Tikhomirov, Nucl. Instrum. Meth. B309, 30-36 (2013).
[31] J. Beringer *et al.* (Particle Data Group), Phys. Rev. D86, 010001 (2012).
[32] Y. Takabayashi, Yu. L. Pivovarov, T.A. Tukhfatullin, Phys. Lett. A378, 21, 1520 (2014).
[33] E. Bagli and V. Guidi, Nucl. Instrum. Methods B 309, 124 (2013).